

# xTrace: A Facial Expressive Behaviour Analysis Tool for Continuous Affect Recognition

Mani Kumar Tellamekala\*  
mani@blueskeye.com  
Blueskeye AI, UK

Shashank Jaiswal  
shashank@blueskeye.com  
Blueskeye AI, UK

Thomas Smith  
tom@blueskeye.com  
Blueskeye AI, UK

Timur Alamev  
timur@blueskeye.com  
Blueskeye AI, UK

Gary McKeown  
G.McKeown@qub.ac.uk  
Queen's University Belfast, UK

Anthony Brown  
tosh@blueskeye.com  
Blueskeye AI, UK

Michel Valstar  
michel@blueskeye.com  
Blueskeye AI, UK

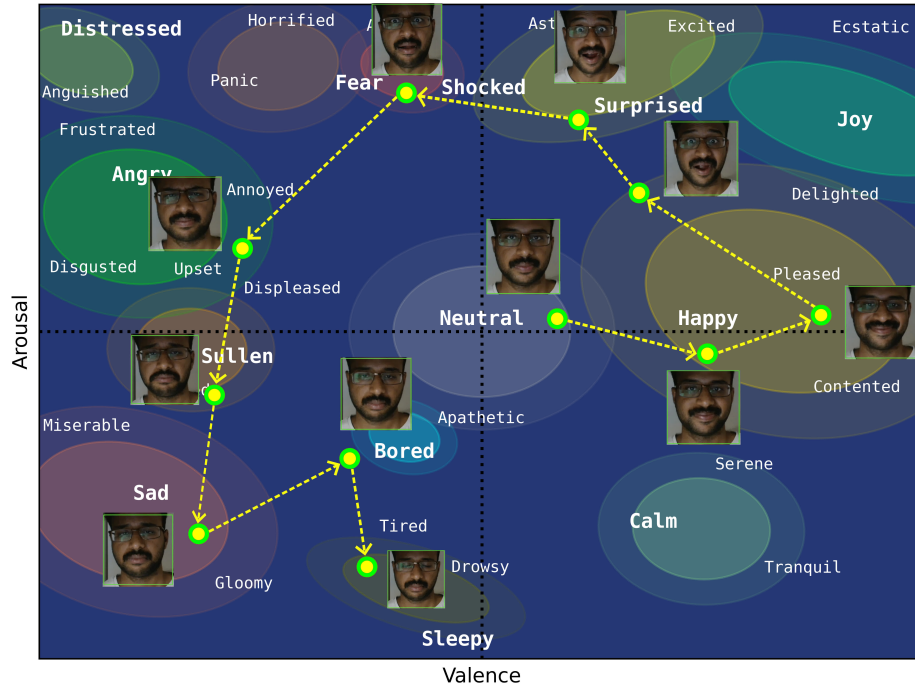


Figure 1: Extensive predictive range of xTrace for continuous affect recognition within the 2D Emotion space

## Abstract

Recognising expressive behaviours in face videos is a long-standing challenge in Affective Computing. Despite significant advancements in recent years, it still remains a challenge to build a robust and reliable system for naturalistic and in-the-wild facial expressive behaviour analysis in real time. This paper addresses two key challenges in building such a system: (1). The paucity of large-scale labelled facial affect video datasets with extensive coverage of the 2D emotion space, and (2). The difficulty of extracting facial video features that are discriminative, interpretable, robust, and computationally efficient. Toward addressing these challenges, we

introduce xTrace, a robust tool for facial expressive behaviour analysis and predicting continuous values of dimensional emotions, namely valence and arousal, from in-the-wild face videos.

To address challenge (1), our affect recognition model is trained on the largest facial affect video data set, containing 450k videos that cover most emotion zones in the dimensional emotion space, making xTrace highly versatile in analysing a wide spectrum of naturalistic expressive behaviours. To address challenge (2), xTrace uses facial affect descriptors that are not only explainable, but can also achieve a high degree of accuracy and robustness with low computational complexity. The key components of xTrace are benchmarked against three existing tools: MediaPipe, OpenFace,

\*Corresponding Author

and Augsburg Affect Toolbox. On an in-the-wild validation set composed of 50k videos, xTrace achieves 0.86 mean CCC and 0.13 mean absolute error values. We present a detailed error analysis of affect predictions from xTrace, illustrating (a). its ability to recognise emotions with high accuracy across most bins in the 2D emotion space, (b). its robustness to non-frontal head pose angles, and (c). a strong correlation between its uncertainty estimates and its accuracy.

## Keywords

Facial Expression Analysis, Dimensional Emotion Recognition, Uncertainty-Aware Affect Estimation

## 1 Introduction

Automatic recognition of facial expressive behaviour is a critical component in enabling empathetic Human-Computer Interactions. During the last three decades, several efforts have been made to build tools for recognising apparent affect or emotion from face videos [10, 18, 21, 28]. Despite the significant progress made so far, robust facial affect recognition in naturalistic conditions is still not a solved problem. Why is it challenging to build such a robust tool capable of handling real-world complexities?

Affective states and their nuances encountered in everyday naturalistic interactions go beyond the seven basic emotions [3]: neutral, happy, angry, sad, disgust, fear, and surprise. Most of the existing methods in the literature [6, 26, 29] and the widely used tools for facial expression analysis (e.g. DeepFace<sup>1</sup>) largely focus on the seven basic emotions, severely limiting their applicability to real-world scenarios. Most importantly, due to its discrete nature, the basic emotion model fails to capture the richness of emotional expressions encountered in naturalistic interactions. The dimensional model of continuous emotions [19] is considered one solution to address this limitation. As shown in Figure 1, the dimensional model has the ability to describe a wide range of emotions. It does so by representing the affective states as points living in a two-dimensional Euclidean space constructed by the dimensions: Valence (positive vs. negative) and Arousal (calm vs. excited). Thus, the dimensional emotion model makes it possible to estimate facial affect as continuous values in the 2D emotion space and time.

The dimensional model has received a lot of interest in Affective Computing in recent years [4, 17, 27], however, its application in real-world systems is still very limited. One main reason for this is the paucity of large-scale in-the-wild affect-labelled video datasets for facial expressive behaviour analysis. Existing video datasets are relatively small in scale, with limited coverage of affective states in the 2D emotion space. For example, the Aff-wild-2 dataset [11] has almost no data for the low-arousal quadrants (see Figure 3). As a result, the models trained and validated on such datasets, despite showing impressive accuracy levels, offer limited practical use in recognising a wide range of apparent emotions. In this work, we introduce a novel facial expressive behaviour analysis tool, xTrace, a versatile tool for recognising expressed facial affect in real time. Towards addressing the aforementioned limitations of the existing video affect datasets, we use the largest in-the-wild facial video affect dataset composed of 450k in-the-wild face videos to train the continuous affect recognition model in xTrace. As a result,

this model shows wide predictive range of affective states in the dimensional emotion space, as shown in Figure 1.

From a system building point of view, to make xTrace robust, accurate, and reliable in real-world applications, we incorporate the following factors into its design:

- (1) A wide predictive coverage in the 2D emotion space
- (2) The ability to leverage long-range temporal video context for reliable emotion predictions
- (3) The use of explainable and interpretable features for traceability and transparency to mitigate model bias risks
- (4) Robustness to partial facial occlusions (induced by non-frontal head pose angles and external objects such as glasses, facial hair, etc.)
- (5) The ability to output predictive uncertainty estimates for the benefit of downstream tasks
- (6) Invariance to input image sensors (RGB vs. Near-Infra Red)

The affect recognition model in xTrace is extensively evaluated w.r.t. its input feature accuracy, its output accuracy variations across the emotion space with varying levels of granularity, its robustness to occlusions, and the quality of its predictive uncertainty estimates. The key components of xTrace, 2D face alignment, Action Unit (AU) recognition, and affect recognition, are extensively benchmarked against existing tools such as MediaPipe [14], OpenFace [23] and Augsburg Affect Toolbox [16]. The evaluation results show that xTrace outperforms these tools by significant margins on in-the-wild validation datasets.

In summary, the key merits of xTrace are as follows:

- Demonstrates high prediction accuracy across all key affective states by achieving an average CCC of 0.86.
- Shows minimal accuracy degradation in the presence of facial occlusions induced by non-frontal head pose angles and external objects.
- Uses explainable and interpretable facial affect descriptors: uncertainty-aware facial landmarks and AU intensities.
- Outputs predictive uncertainty estimates so that downstream tasks can decide when to trust affect predictions.

## 2 System Architecture

Taking a sequence of  $N$  consecutive video frames as input, xTrace outputs a sequence of VA predictions per frame and their corresponding uncertainty estimates. As illustrated in Figure 2, the end-to-end system architecture of xTrace is composed of three main modules: (1). *Uncertainty-aware landmark regression* (2). *AU intensity estimation* and (3). *Temporal affect regression*. In this section, we first explain the rationale behind the key underlying design choices of xTrace and then describe each of these modules in detail.

### 2.1 Key System Design Choices

**Affect Feature Descriptors** Broadly, there are two categories of facial affect feature sets: High-Level Descriptors (HLDs) and Deep Visual Descriptors. The former set of descriptors is derived from pre-defined facial geometry information and some standard facial actions. The latter set of features are inferred directly from cropped face images and/or image sequences using an end-to-end deep neural network trained using large amounts of affect-labelled data. A commonly used set of HLDs in the literature on facial affect

<sup>1</sup><https://github.com/serengil/deepface>

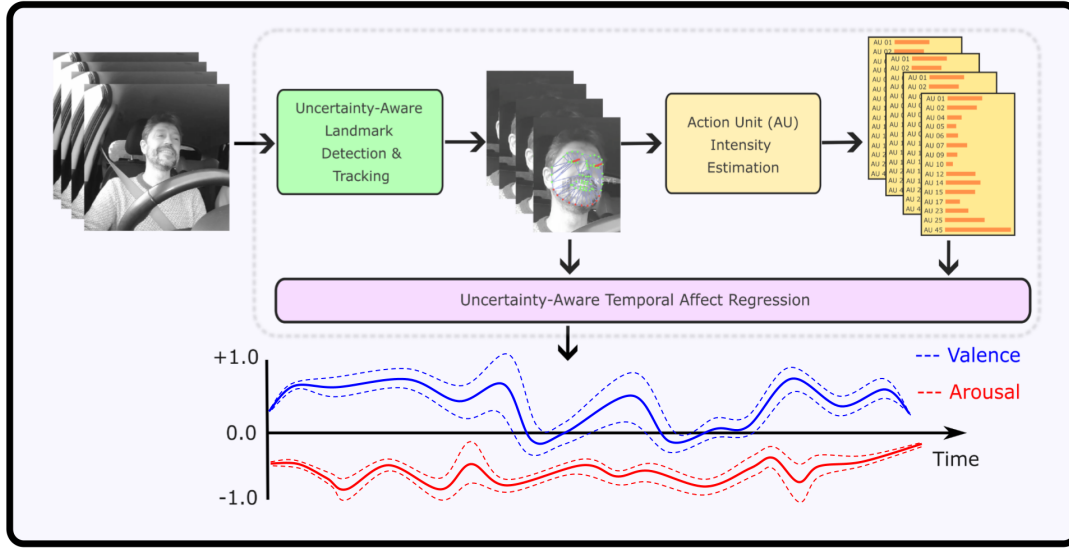


Figure 2: The end-to-end pipeline of xTrace for temporal valence and arousal estimation from face videos

analysis are facial landmarks [7] and facial action units [2]. With the advent and success of deep representation learning in the past ten years, various deep visual features have been explored for facial affect recognition tasks. EmoNet [27] is a state-of-the-art approach based on deep visual features jointly learnt deep visual features for landmark regression and affect recognition.

As facial affect descriptors in xTrace, we chose to use HLDs, particularly 2D facial landmark features, their confidence scores and AU intensities over deep visual features for the following reasons:

**Explainability and Interpretability.** Unlike deep visual features, HLDs are easy to explain and interpret given that they are standardised affect descriptors strongly grounded in localised facial appearance changes. For example, AU intensity features capture atomic movements of facial muscles and their temporal dynamics. When used as input features, AU features render transparency which deep visual features lack due to their black box and hierarchically compositional nature. For example, humans easily interpret the meaning of specific facial actions like a brow-raise (AU1, AU2) or a smile (AU12), whereas deep visual features often lack such direct human interpretability. Given this advantage with HLDs, we can trace the affect recognition model’s emotion predictions back to its corresponding input features, and precisely attribute them to visible appearance changes in different face regions. This traceability is particularly helpful in characterising the model’s failure cases and improving the model’s accuracy and robustness.

**Efficient use of labelled affect data.** When training an end-to-end model for affect recognition from face videos, the labelled data are used for supervision for two subtasks: learning per-frame visual features from face image pixels and learning temporal dynamics that are relevant to affect prediction. The former task involves distilling facial expression visual features that are robust to nuisance

factors such as changes in head pose, lighting, occlusions, etc. To achieve such a high degree of robustness, it requires large amounts of affect-labelled data or sophisticated pre-training techniques (e.g., SwaV [1]) or joint-learning methods (e.g., EmoNet [27]). To achieve high affect recognition accuracy, it also requires large amounts of temporal variations in affect labels in training sets, to learn temporal dynamics of the facial features. Achieving both these objectives requires enormously large amounts of affect-labelled data, obtaining which is prohibitively expensive due to the requirement of trained human annotators for this task. To efficiently use the labelled data, in this work we chose HLDs whose models are trained to be robust to changes in head-pose angles, lighting, and occlusions. Thus, in the proposed system all the affect-labelled data gets mainly used for learning the temporal dynamics of affect labels.

**Leveraging long-range temporal context.** Considering how crucial temporal elements are in facial emotions, the use of temporal context is known to be critical to improving the accuracy of affect recognition systems [15, 21, 25]. Due to their high computational complexity and large feature dimensionality, end-to-end architectures used for deep visual feature extraction typically use short temporal sequences at training time, thus limiting the amount of temporal context they can leverage effectively. In contrast, given the HLDs’ low-dimensionality and the computationally light-weight regression model used, the affect recognition model in xTrace can make use of long-range temporal context (e.g. 4 to 5 seconds) for predicting VA values with better accuracy levels.

**Low computational complexity and inference latency.** The HLD-based affect recognition model is significantly less complex in its computational requirements, as it focuses mainly on temporal dynamics and offloads feature extraction to the ‘backbone’ models, which are landmark regression and AU estimation in xTrace. When

these backbone models are heavily optimised for low inference complexity and latency, the overall system is much lighter compared to an end-to-end model such as EmoNet. It is also worth noting that unlike the end-to-end architectures, the architecture of xTrace makes it much easier to distribute its modules to different compute processing units on low-end embedded devices.

**Agnostic to low-level image characteristics.** This is a critical requirement to make an affect recognition system invariant to changes in image acquisition process. For example, an end-to-end model trained on RGB images is likely to fail when applied to Near-Infrared (NIR) images of arbitrary wavelengths. This could be due to the dependence of deep visual features on low-level pixel statistics. Due to this limitation, an additional model fine-tuning effort may be required when there is a change in the image acquisition steps. In xTrace, by making the models responsible for HLDs robust to such low-level pixel patterns, the affect recognition model is made agnostic to any low-level image characteristics.

## 2.2 Affect Regression Outputs

**Time- and value-continuous predictions of affect.** The affect regression model in xTrace is a sequence-to-sequence mapping model that takes a sequence of HLDs per frame as input and outputs a sequence of valence and arousal estimates. By mapping each frame to its corresponding continuous-valued vector in the 2D emotion space, this fine-grained approach allows us to make full use of the emotion representation capacity of the dimensional affect model. Also, by outputting per-frame affect vectors, this model captures transient and sudden changes in affective states over time. This level of spatio-temporal granularity broadens the applicability of xTrace for a broad spectrum of behavioural analysis tasks.

**Sampling-free predictive uncertainty estimates of affect.** In addition to the point-wise affect predictions, xTrace also outputs three types of predictive uncertainty estimates of affect: Epistemic, Aleatoric, and cumulative [5]. Most importantly, unlike other existing methods [8, 24], it does so in a sampling-free manner, i.e., without requiring multiple forward passes through the model at inference time. This ability is important in obtaining uncertainty estimates with limited computational resources at inference time. Predictive uncertainties are essential for downstream applications to decide when they can or cannot trust the affect predictions. The three types of affect uncertainty output from xTrace have specific use cases. Epistemic uncertainty or model uncertainty allows the system to flag and collect out-of-distribution inputs and guide training data collection in later model update iterations. This feature is critical to continuously improve the coverage, accuracy, and robustness of the system over time. The aleatoric or data uncertainty captures the stochastic noise inherent in the input video. For example, when there is strong illumination on the face making it difficult to read the expression, the aleatoric uncertainty is expected to be high. When implemented in real-world applications, having access to this component of uncertainty can guide any potential automated interventions to improve the quality of face video. The cumulative uncertainty captures both epistemic and aleatoric components and

it can be made available to a downstream task to decide how reliable the affect predictions are for a given input.

## 2.3 Module Descriptions

**Uncertainty-Aware Landmark Detection and Tracking.** This module takes a video frame as input and outputs (a). a binary label for face shape validity (b). a 2D array of 68 landmark coordinates in iBUG format [20] and (c). a 1D array of landmark-wise uncertainty estimates. This module uses an edge-friendly CNN architecture with three output heads to jointly predict these three outputs. This CNN model is trained to be robust to in-the-wild facial appearances, on an internal curated face image dataset containing 650k RGB and NIR images labelled with 68 landmarks and their visibility scores.

Note that the face-shape validity output is learned in an unsupervised fashion, whereas the landmark-wise uncertainty values are learned using explicit supervision. If the predicted face shape validity label is false for the current frame in the buffer, its corresponding affect features (both landmarks and AUs) are set to zeros and the next video frame in the buffer gets processed. If not, the predicted landmarks are used to preprocess the input to the AU intensity estimation module.

This module first extracts the face crop from the video frame using the bounding box computed from the previous frame's landmark coordinates. In case there is no previous frame or its predicted face shape validity is False, the bounding box is obtained from a face detection model heavily optimised for low inference latency and high detection accuracy on the edge devices.

**AU Intensity Estimation** model takes an image of similarity-transformed face crop as input and outputs a 15-dimensional AU intensity vector. The predicted AU intensity outputs are continuous values in the range [0,5]; 0 indicates no activation and 5 indicates maximum activation. Similar to the landmark detection and tracking model, this module also uses an edge-friendly CNN architecture for compute-efficient model inference. By training on an internally curated dataset that contains 2.4 million in-the-wild facial appearances, the AU model is made robust to the presence of partial occlusions and non-uniform illumination.

**Uncertainty-Aware Temporal Affect Regression** receives a sequence of temporal features, and outputs a sequence of VA predictions and their corresponding estimates of the epistemic, aleatoric, and cumulative uncertainty components. VA predictions are continuous values in the range [-1.0, 1.0], and their corresponding uncertainty estimates are clamped to the range [0, 1.0]. The input features to this model are prepared by normalising per-frame landmark coordinates and their corresponding uncertainty scores, and normalised AU intensity values. These normalised per-frame features are filled into a temporal buffer in a sliding window manner.

## 3 Video Datasets for Facial Affect Recognition

**Limitations of Existing Datasets.** SEWA [13] and Aff-wild-2 [11] are two prominent in-the-wild video datasets that are used to train and evaluate most existing facial affect recognition models. These datasets enabled numerous advancements in affect recognition [10],

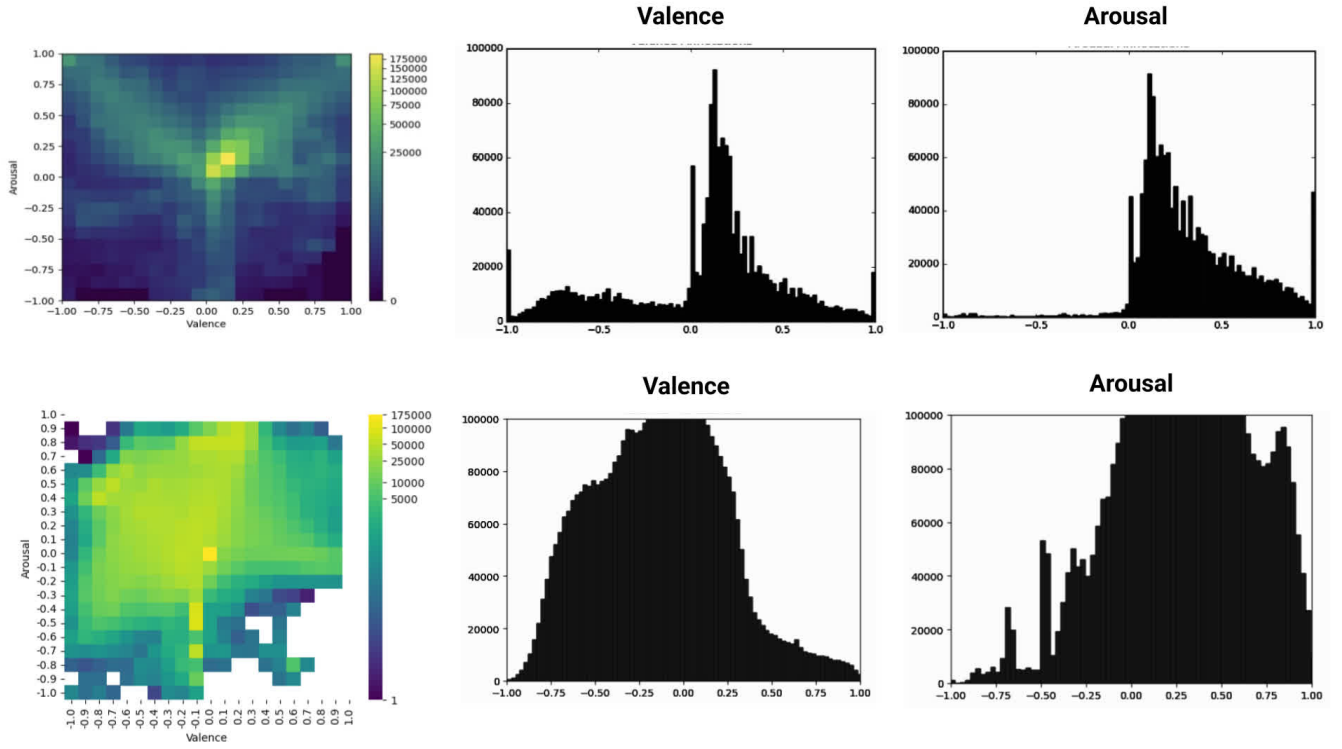


Figure 3: Comparison of emotion label distributions between the Aff-Wild2 dataset [10](top) and the xTrace dataset (bottom).



Figure 4: Sample face images from the xTrace VA dataset

especially the Aff-wild-2 dataset through a series of ABAW challenges [9, 12]. However, they are still relatively small-scale datasets: SEWA contains 538 videos collected from 398 subjects, and Aff-wild-2 is composed of 594 videos from 584 subjects. Considering the complexity of naturalistic affect recognition as a learning task, such small-scale datasets may not be sufficient to cover the variations encountered in naturalistic and in-the-wild emotional expressions. Another key limitation of these datasets is their limited coverage of the Valence and Arousal space. For example, as shown in Figure 3 (a), the label distributions of Aff-wild-2 clearly show insufficient coverage of the affect space. To make the proposed facial affect recognition model in this work robust to real-world variations and cover the 2D emotion space as extensively as possible, we used a well-curated large-scale video dataset constructed from various in-house collected and curated face videos.

**Expressive Video Clips Curation.** A set of 450k short video clips is curated from various in-house collected and in-the-wild face

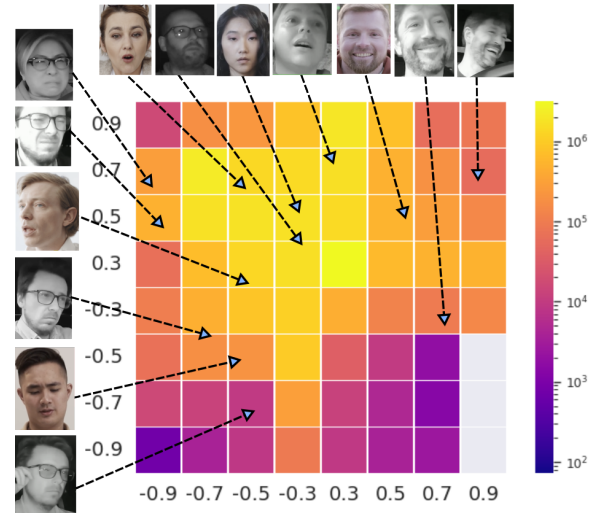


Figure 5: VA label distribution in the xTrace training dataset

video datasets. These datasets were sourced from 8.5k subjects. For example, Figure 4 shows some RGB face images sampled from in-the-wild settings. The duration of the extracted short video clips varies in the range of 3 to 5 seconds. This video set also contains a significant proportion of NIR face videos captured in in-lab and driving (in-car) settings. To make sure that the low-arousal quadrants in the emotion space have a representative number of examples in this

dataset, video clips sourced from an internal collected drowsiness dataset are also included. This dataset is partitioned into train and validation sets in a subject-independent fashion, resulting in 400k clips for training and 50k clips for validation and testing purposes. **VA Annotation.** Considering the prohibitively expensive nature of trace-based per-frame VA annotation approaches, we employed a semi-automated annotation methodology to obtain per-clip VA emotion labels in a scalable approach. In this method, we used a simple web interface tool for single-point VA annotation in which each video clip is labelled with a point in the 2D emotion space. Compared to the label distributions of the Aff-wild-2 datasets, as shown in Figure 3 (b), the overall label distribution of this dataset has much better coverage in the VA space. Representative frames sampled from some example training video clips with different VA values are illustrated in Figure 5.

**Inter-Rater Disagreement Analysis.** To evaluate the quality of VA labels obtained using the single-point annotation method described above, we performed an inter-rater disagreement analysis. For this purpose, we extracted a subset of 30k video clips annotated by at least three human raters. Since the labels annotated here are not traces but single points, instead of the standard correlation measures, we adopted a simple weighted mean absolute error (WMAE) method for measuring the inter-rater disagreement scores. Here, the weight values used in the MAE function are derived from the inverted distance values between the corresponding points. Given three VA annotations for a video clip, we computed WMAE scores using the weights derived inter-rater reliability scores [22] calculated for each annotator. On this 30k video subset, the average WMAE values obtained for valence and arousal dimensions are 0.17 and 0.19 respectively. These low WMAE values indicate good inter-rater agreement levels of the annotated VA labels.

## 4 Evaluation Results

### 4.1 Affect Feature Descriptor Evaluation

**Uncertainty-Aware Landmark Detection Evaluation** results are presented in Table 1. For this evaluation, we used an internally curated validation dataset composed of 39k in-the-wild RGB and NIR images. Both metrics, Area Under Curve (AUC) and Normalised Mean Error (NME), clearly show that the landmark detection model in xTrace achieves noticeably better point localisation accuracy despite its low computational complexity. Figure 8 illustrates the ability of landmark-wise uncertainty estimates in detecting occluded facial regions, by comparing **visible** and **occluded** landmarks.

Model	RGB Set		NIR Set	
	NME↓	AUC↑	NME↓	AUC↑
OpenFace 2.2.0 [23]	7.03	55.46	4.56	60.29
MediaPipe [14]	4.36	55.77	6.62	46.69
xTrace	<b>1.59</b>	<b>88.72</b>	<b>1.12</b>	<b>89.68</b>

Table 1: Landmark detection evaluation results

**AU Intensity Estimation Evaluation** results are shown in Table 2, in terms of AU-wise and mean Intra-Class Correlation (ICC)

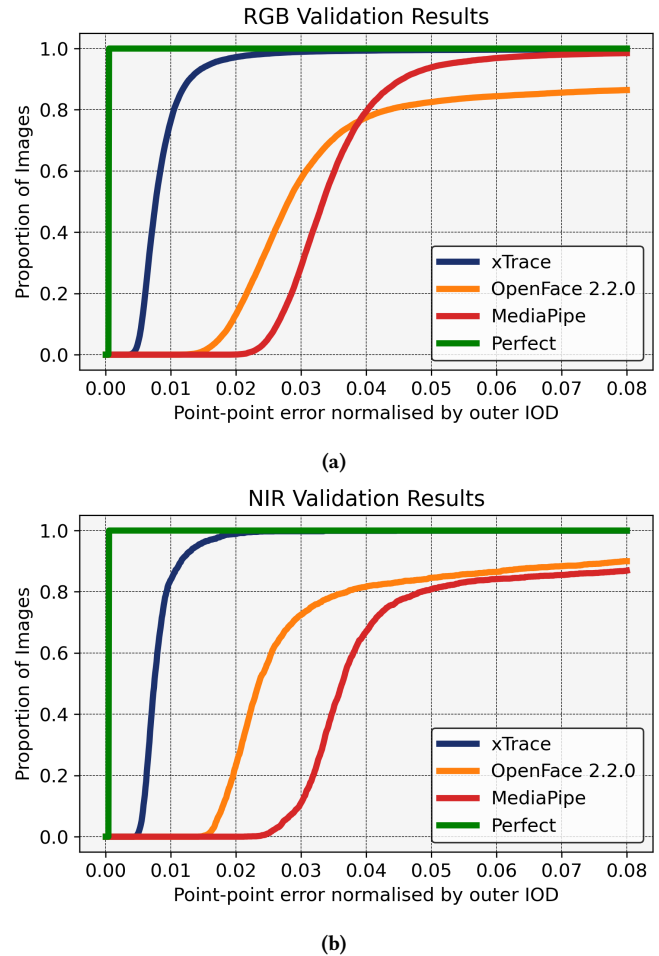


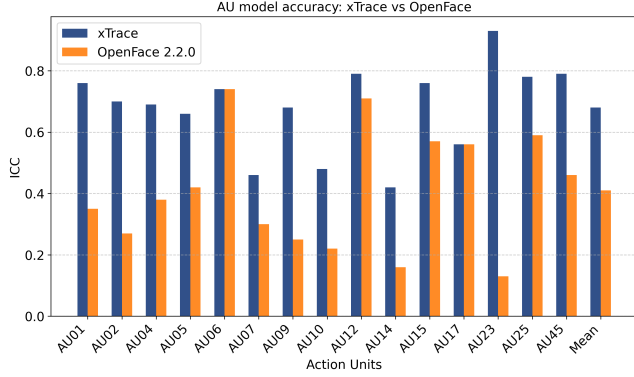
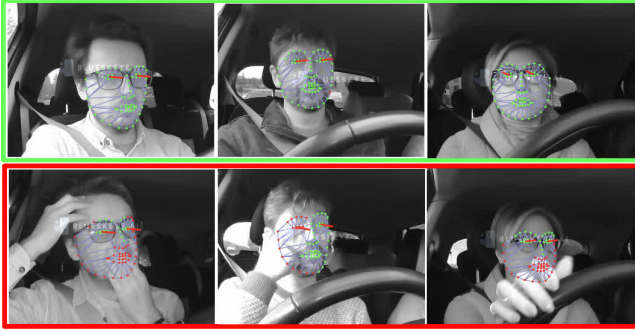
Figure 6: Cumulative Error Distribution (CED) plots of landmark detection models on (a) RGB and (b) NIR images.

scores. This in-house evaluation set contains 175k RGB and NIR face images annotated with AU intensity values of 15 AUs. Except for two AUs (07 and 14), for all other AUs the ICC scores are above 0.5. Overall, these high ICC scores clearly indicate the strong predictive accuracy of the AU intensity model used in xTrace, and it outperformed OpenFace by 27% in terms of the mean ICC score.

### 4.2 Affect Recognition Evaluation

**Overall VA Accuracy Evaluation Results** across the 2D affect space are presented in Figure 9 in terms of two standard evaluation metrics [10, 27]: Concordance Correlation Coefficient (CCC) and Mean Absolute Error (MAE). While CCC captures the overall agreement between the model predictions and ground truth labels of all the test samples, MAE is computed between individual (per-frame) predictions and then averaged for all the samples. In total, this internally curated validation set contains 5 million frames from 50k in-the-wild test videos. This validation set is carefully constructed to cover as many bins as possible in the 2D affect space (see the sample distribution maps in Figure 10.b.). The CCC scores

AU	01	02	04	05	06	07	09	10	12	14	15	17	23	25	45	Avg.
<b>OpenFace 2.2.0</b>	0.35	0.27	0.38	0.42	0.74	0.30	0.25	0.22	0.71	0.16	0.57	0.56	0.13	0.59	0.46	0.41
<b>xTrace</b>	0.76	0.70	0.69	0.66	0.75	0.47	0.68	0.53	0.79	0.42	0.76	0.54	0.93	0.78	0.79	<b>0.68</b>

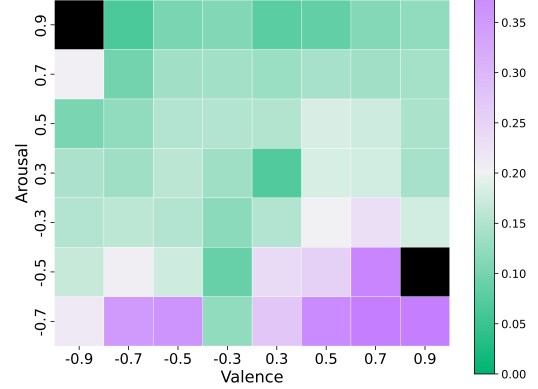
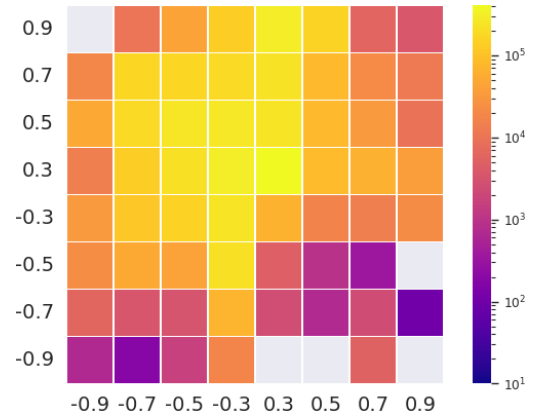
**Table 2: Evaluation results of the AU intensity estimation model in xTrace and comparison with OpenFace 2.2.0**

**Figure 7: AU model accuracy comparison with OpenFace**

**Figure 8: Landmark uncertainty estimates quality in xTrace**

(a). Number of Test Frames		(b). CCC Scores		(c). MAE Values	
Total frame count: 5,085,900		Overall V: 0.83 Overall A: 0.89		Overall V: 0.14 Overall A: 0.12	
2,192,976	1,770,150	V: 0.68 A: 0.77	V: 0.64 A: 0.92	V: 0.14 A: 0.13	V: 0.14 A: 0.09
984,676	138,098	V: 0.79 A: 0.52	V: 0.57 A: 0.40	V: 0.11 A: 0.17	V: 0.25 A: 0.16

**Figure 9: xTrace VA evaluation results**

and MAE values for both valence and arousal clearly illustrate the strong predictive accuracy of the affect recognition model in xTrace.

**Quadrant-wise VA Evaluation Results** are presented in Figure 9: (a). number of test frames (b). CCC scores and (c). MAE values for each quadrant. It is important to note that this evaluation set contains significantly more frames in the positive arousal quadrants


**(a) MAE distribution map on the VA validation set**

**(b) Sample distribution map of the VA validation set**
**Figure 10: Fine-grained VA evaluation results of xTrace**

Head Pose	CCC↑		MAE↓	
	Vale.	Arou.	Vale.	Arou.
Frontal	0.86	0.86	0.16	0.15
Yaw +30 deg	0.85	0.85	0.18	0.15
Yaw -30 deg	0.88	0.82	0.15	0.16
Yaw +60 deg	0.84	0.84	0.19	0.15
Yaw -60 deg	0.87	0.78	0.16	0.18
Pitch +25 deg	0.86	0.84	0.17	0.15
Pitch -25 deg	0.83	0.84	0.18	0.16

**Table 3: VA evaluation with varying head pose angles**

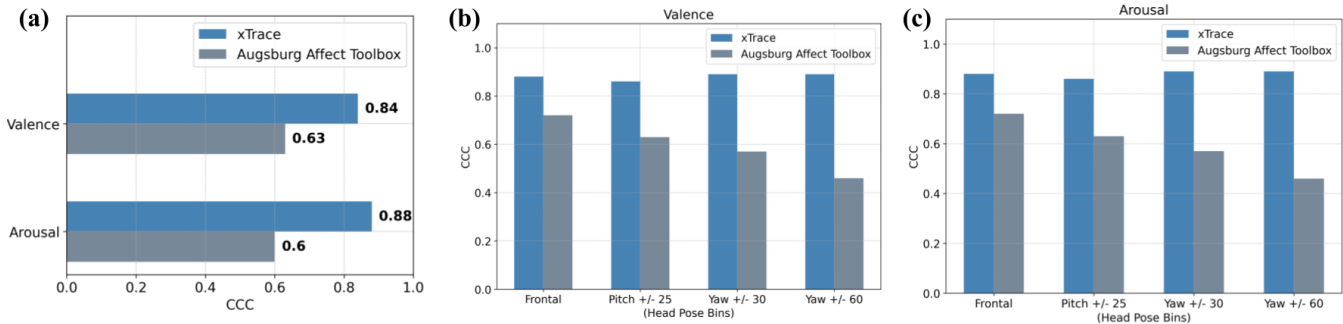


Figure 11: xTrace vs. Augsburg Affect Toolbox: (a). overall CCC and (b) and (c). robustness to non-frontal head pose angles.

compared to the negative arousal quadrants. This imbalanced label distribution can also be seen in the training set (see Figure 3).

The CCC scores and MAE values show the differences in the model accuracy across the four quadrants. For example, the valence CCC is the highest for the negative valence and negative arousal quadrant. However, the arousal CCC is the highest for the positive valence and positive arousal quadrant. In particular, in the case of arousal CCC the differences between the quadrants are more noticeable compared to the valence dimension. Interestingly, in the MAE values, the trends in cross-quadrant differences are a bit different compared to the CCC scores. These imbalances in model performance across different quadrants may be partly due to the imbalances in the training dataset. Also, it is worth noting that the visual modality (i.e., face videos) is known to be relatively less informative for arousal than valence.

More fine-grained VA evaluation results (MAE values) are presented in Figure 10, along with the sample distribution map of the evaluation set. As computing CCC scores makes less sense in the case of fine-grained bins, we used MAE scores to compare the model’s accuracy across different VA bins. The bins with MAE values below and above human inter-rater disagreement (Weighted MAE) are marked in green and purple colors respectively. This result clearly illustrates that xTrace performs well in most VA bins, except for a few bins in the low-arousal quadrants. It could be due to the limitations of the visual modality in inferring arousal [18].

**VA Accuracy Robustness to Non-Frontal Head Pose** is analysed in Table 3 in terms of the CCC scores and the MAE values. The nonfrontal head pose angles considered in this evaluation cover the yaw bins [+60, +30, 0, +30, -60] and the pitch bins [+25, 0, -25]. For a fair comparison, it is ensured that this internal evaluation set is curated for each pose bin so that it has a roughly equal number of video clips (3k clips per pose bin). Both CCC and MAE values show that the VA model’s accuracy is highly robust to changes in the head pose angles. It is worth noting that even for the yaw +/- 60 degree range, the VA predictive accuracy drop is very low, compared to the frontal bin’s VA accuracy.

**Leave N-in Validation Results of VA Uncertainty** estimates are presented in Table 4. In this evaluation protocol, only N% of the validation examples are considered for evaluation based on how high or low their cumulative uncertainty scores are. The CCC and MAE values that correspond to the ‘Lowest Uncertainty Filter’

Dimension	Metric	Filter Type	Accuracy Trend (N: 25% → 100%)
Valence	CCC	Lowest Uncert.	0.93 ↓ 0.81
		Highest Uncert.	0.61 ↑ 0.81
	MAE	Lowest Uncert.	0.08 ↑ 0.15
		Highest Uncert.	0.21 ↓ 0.15
Arousal	CCC	Lowest Uncert.	0.94 ↓ 0.88
		Highest Uncert.	0.73 ↑ 0.88
	MAE	Lowest Uncert.	0.07 ↑ 0.14
		Highest Uncert.	0.20 ↓ 0.14

Accuracy Trend: Green ↑↓ - Improving accuracy, Red ↑↓ - Degrading accuracy

Table 4: Leave-N-in validation results of VA uncertainty

show how well the model performs when we consider only N% of validation examples with the lowest uncertainty. Similarly, the results of the ‘Highest Uncertainty Filter’ show how worse the model performs when only the examples with the highest uncertainty are considered for evaluation. The trends in the CCC and MAE values in Table 4 for different N values show that the cumulative uncertainty scores are strongly correlated with the predictive accuracy. This strong correlation suggests that we can assess the reliability of xTrace’s affect predictions in downstream applications.

## 5 Conclusion

In this paper, we introduced xTrace, a robust, explainable and computationally lightweight tool for in-the-wild naturalistic facial expressive behaviour analysis. xTrace is trained on a corpus of 450k face videos, the largest video dataset for affect recognition to date. This makes xTrace capable of handling challenges encountered in real-world settings, ranging from subtle and nuanced expressive cues to partial occlusions caused by non-frontal head pose angles, etc. Some key system design choices we made in building xTrace include using Low-Level Descriptors of facial expressions (for model interpretability and compute efficiency), leveraging long-range temporal context (for temporally consistent affect predictions) and outputting sampling-free uncertainty estimates (for reliability in downstream applications). Through extensive benchmarking of xTrace’s components against existing tools such as MediaPipe, OpenFace and Augsburg Affect Toolbox, we demonstrated its superior accuracy in face alignment, AU intensity estimation and continuous affect recognition tasks. We believe xTrace will accelerate the adoption of facial affect recognition in a wide range of real-world applications

supporting empathetic human-computer interactions.

**Safe and Responsible Innovation.** The proposed tool for facial expressive behavior analysis has several real-world applications to support empathetic Human-Computer interactions. Towards addressing risks with existing end-to-end AI tools for facial expression analysis, the tool proposed in this work is made more explainable by using High-Level Descriptors of facial expressions. We explicitly recognise that facial expressions are influenced by cultural backgrounds and are not perfect indicators of internal states. Responsible development requires acknowledging these limitations and ensuring data privacy. We commit to promoting ethical guidelines and responsible practices for the application of this tool.

## References

- [1] Mathilde Caron, Ishan Misra, Julien Mairal, Priya Goyal, Piotr Bojanowski, and Armand Joulin. 2020. Unsupervised learning of visual features by contrasting cluster assignments. *NeurIPS* (2020), 9912–9924.
- [2] Paul Ekman. 1977. Facial action coding system. (1977).
- [3] Paul Ekman. 1999. Basic emotions. *Handbook of cognition and emotion* 98, 45–60 (1999), 16.
- [4] Hatice Gunes, Björn Schuller, Maja Pantic, and Roddy Cowie. 2011. Emotion representation, analysis and synthesis in continuous space: A survey. In *2011 IEEE International Conference on Automatic Face & Gesture Recognition (FG)*. IEEE, 827–834.
- [5] Eyke Hüllermeier and Willem Waegeman. 2021. Aleatoric and epistemic uncertainty in machine learning: An introduction to concepts and methods. *Machine Learning* 110, 3 (2021), 457–506.
- [6] Xingxun Jiang, Yuan Zong, Wenming Zheng, Chuangao Tang, Wanchuang Xia, Cheng Lu, and Jiateng Liu. 2020. Dfew: A large-scale database for recognizing dynamic facial expressions in the wild. In *Proceedings of the 28th ACM international conference on multimedia*. 2881–2889.
- [7] Xin Jin and Xiaoyang Tan. 2017. Face alignment in-the-wild: A survey. *Computer Vision and Image Understanding* 162 (2017), 1–22.
- [8] Alex Kendall and Yarin Gal. 2017. What uncertainties do we need in bayesian deep learning for computer vision? *arXiv preprint arXiv:1703.04977* (2017).
- [9] Dimitrios Kollias, Attila Schulc, Elnar Hajiyeve, and Stefanos Zafeiriou. 2020. Analysing Affective Behavior in the First ABAW 2020 Competition. In *IEEE FG*. 637–643.
- [10] Dimitrios Kollias, Panagiotis Tzirakis, Alan Cowen, S Zafeiriou, I Kotsia, Eric Granger, Marco Pedersoli, SL Bacon, Alice Baird, C Gagne, et al. 2025. Advancements in Affective and Behavior Analysis: The 8th ABAW Workshop and Competition. (2025).
- [11] Dimitrios Kollias and Stefanos Zafeiriou. 2018. Aff-Wild2: Extending the Aff-Wild Database for Affect Recognition. *arXiv preprint:1811.07770* (2018).
- [12] Dimitrios Kollias and Stefanos Zafeiriou. 2021. Analysing Affective Behavior in the Second ABAW2 Competition. In *ICCV*. 3652–3660.
- [13] Jean Kossaifi, Robert Walecki, Yannis Panagakis, Jie Shen, Maximilian Schmitt, Fabien Ringeval, Jing Han, Vedhas Pandit, Antoine Toisoul, Björn Schuller, et al. 2019. SEWA DB: A rich database for audio-visual emotion and sentiment research in the wild. *IEEE TPAMI* 43, 3 (2019), 1022–1040.
- [14] Camillo Lugaresi, Jiuqiang Tang, Hadon Nash, Chris McClanahan, Esha Ubowaja, Michael Hays, Fan Zhang, Chuo-Ling Chang, Ming Guang Yong, Juhyun Lee, et al. 2019. Mediapipe: A framework for building perception pipelines. *arXiv preprint arXiv:1906.08172* (2019).
- [15] Hongying Meng, Nadia Bianchi-Berthouze, Yangdong Deng, Jinkuang Cheng, and John P Cosmas. 2015. Time-delay neural network for continuous emotional dimension prediction from facial expression sequences. *IEEE Trans. on Cybern.* 46, 4 (2015), 916–929.
- [16] Silvan Mertes, Dominik Schiller, Michael Dietz, Elisabeth André, and Florian Lingens. 2024. The AffectToolbox: Affect Analysis for Everyone. *arXiv preprint arXiv:2402.15195* (2024).
- [17] Mihalios A Nicolaou, Hatice Gunes, and Maja Pantic. 2011. Continuous prediction of spontaneous affect from multiple cues and modalities in valence-arousal space. *IEEE TAC* 2, 2 (2011), 92–105.
- [18] Maja Pantic and Leon J. M. Rothkrantz. 2000. Automatic analysis of facial expressions: The state of the art. *IEEE Transactions on pattern analysis and machine intelligence* 22, 12 (2000), 1424–1445.
- [19] James A Russell. 1980. A circumplex model of affect. *Journal of personality and social psychology* 39, 6 (1980), 1161.
- [20] Christos Sagonas, Epameinondas Antonakos, Georgios Tzimiropoulos, Stefanos Zafeiriou, and Maja Pantic. 2016. 300 faces in-the-wild challenge: Database and results. *Image and vision computing* 47 (2016), 3–18.
- [21] Enrique Sanchez, Mani Kumar Tellamekala, Michel Valstar, and Georgios Tzimiropoulos. 2021. Affective Processes: stochastic modelling of temporal context for emotion and facial expression recognition. In *CVPR*. 9074–9084.
- [22] P.E. Shrout and J.L. Fleiss. 1979. Intraclass correlations: uses in assessing rater reliability. *Psychological bulletin* (1979).
- [23] Baltrusaitis Tadas, Zadeh Amir, Lim Yao Chong, and Morency Louis-Philippe. 2018. Openface 2.0: Facial behavior analysis toolkit. In *13th IEEE International Conference on Automatic Face & Gesture Recognition*.
- [24] Mani Kumar Tellamekala, Timo Giesbrecht, and Michel Valstar. 2022. Dimensional affect uncertainty modelling for apparent personality recognition. *IEEE Transactions on Affective Computing* 13, 4 (2022), 2144–2155.
- [25] Mani Kumar Tellamekala and Michel Valstar. 2019. Temporally Coherent Visual Representations for Dimensional Affect Recognition. In *ACII*. 1–7.
- [26] Yingli Tian, Takeo Kanade, and Jeffrey F Cohn. 2011. Facial expression recognition. In *Handbook of face recognition*. Springer, 487–519.
- [27] Antoine Toisoul, Jean Kossaifi, Adrian Bulat, Georgios Tzimiropoulos, and Maja Pantic. 2021. Estimation of continuous valence and arousal levels from faces in naturalistic conditions. *Nature Machine Intelligence* 3, 1 (2021), 42–50.
- [28] Michel Valstar and Maja Pantic. 2006. Fully automatic facial action unit detection and temporal analysis. In *CVPR workshop*. IEEE, 149–149.
- [29] Yan Wang, Yixuan Sun, Yiwen Huang, Zhongying Liu, Shuyong Gao, Wei Zhang, Weifeng Ge, and Wenqiang Zhang. 2022. Ferv39k: A large-scale multi-scene dataset for facial expression recognition in videos. In *Proceedings of the IEEE/CVF conference on computer vision and pattern recognition*. 20922–20931.